Potential role of nuclear translocation of glyceraldehyde-3-phosphate dehydrogenase in apoptosis and oxidative stress

Zubin Dastoor and Jean-Luc Dreyer
Institute of Biochemistry, University of Fribourg, CH-1700 Fribourg, Switzerland
*Author for correspondence (e-mail: jean-luc.dreyer@unifr.ch)

Accepted 13 February 2001
Journal of Cell Science 114, 1643-1653 © The Company of Biologists Ltd

SUMMARY

Recent studies indicating a role of glyceraldehyde-3-phosphate dehydrogenase (GAPDH) in apoptosis or oxidative stress has been reported. Using confocal laser-scanning microscopy, we have investigated the cellular distribution of GAPDH in central nervous system (CNS)-derived cells (neuroblastoma mNB41A3), in non-CNS derived cells (R6 fibroblast) and in an apoptosis-resistant Bcl2 overexpressing cell line (R6-Bcl2). Induction of apoptosis by staurosporine or MG132 and oxidative stress by H_2O_2 or FeCN enhanced the nuclear translocation of endogenous GAPDH in all cell types, as detected by immunocytochemistry. In apoptotic cells, GAPDH expression is three times higher than in non-apoptotic cells. Consistent with a role for GAPDH in apoptosis, overexpression of a GAPDH-green fluorescent protein (GAPDH-GFP) hybrid increased nuclear import of GAPDH-GFP into transfected cells and the number of apoptotic cells, and made them more sensitive to agents that induce apoptosis. Bcl2 overexpression prevents nuclear translocation of GAPDH and apoptosis in untransfected cells, but not in transfected cells that overexpress GAPDH-GFP. Our observations indicate that nuclear translocation of GAPDH may play a role in apoptosis and oxidative stress, probably related to the activity of GAPDH as a DNA repair enzyme or as a nuclear carrier for pro-apoptotic molecules.

Key words: Apoptosis, Confocal laser-scanning microscopy, Glyceraldehyde-3-phosphate dehydrogenase, Nuclear import, Oxidative stress

INTRODUCTION

Glyceraldehyde-3-phosphate dehydrogenase (GAPDH) is a central glycolytic protein with pivotal role in energy production. However studies have demonstrated that GAPDH or some of its isoforms (>200; Arcari et al., 1989) display a number of activities that are unrelated to its glycolytic function, e.g. phosphotransferase/kinase activity, autophosphorylation or phosphorylation of other proteins, thus acting as a cellular kinase (Kawamoto and Caswell, 1986). It acts as a tubulin-binding protein, catalyzing tubulin polymerization into microtubules (Durrieu et al., 1987; Muronetz et al., 1994), and facilitates membrane fusion in a highly plasmenylethanolamine- and cholesterol-specific manner (Glaser and Gross, 1995) or displays Ca^{2+}-dependent fusogen activity (Hessler et al., 1998). However, GAPDH also acts as a target of nitric oxide (Brune and Lapetina, 1996) or a binding protein for nucleic acids. It has been identified as a specific mRNA-binding protein that interacts with 5′-UTR or 3′-UTR mRNA sequences important for translational regulation of gene expression (Nagy and Rigby, 1995; Schultz et al., 1996), as a DNA binding protein, acting as a non-histone nuclear protein implicated in enhancement of gene expression (Morgenegg et al., 1986), and as a nuclear tRNA export protein (Singh and Green, 1993). It has been further identified as a uracil DNA glycosylase (Meyer-Siegler et al., 1991) and as an Ap_4A-binding protein (Baxi and Vishwanatha, 1995), which implies that it has a role in DNA replication and repair. In turn, it is regulated by protein kinase C, epidermal growth factor kinase and Ca^{2+}/calmodulin-dependent protein kinase II (Ashmarina et al., 1988; Reiss et al., 1996).

A role in apoptosis was initially demonstrated in cerebellar granular cells (CGCs) (Ishitani et al., 1998; Ishitani et al., 1996; Sunaga et al., 1995). Mature CGCs undergo an age-induced apoptotic death, associated with enhanced expression of a 38 kDa protein, identified as GAPDH. GAPDH is localized in the nuclear compartment in cells that undergo apoptosis, and antisense oligodeoxyribonucleotides suppress the accumulation of GAPDH before apoptosis (Ishitani et al., 1998; Saunders et al., 1999; Sawa et al., 1997). Furthermore, GAPDH could be the target of anti-apoptotic compounds, e.g. CGP 3466 and R-(–)-deprenyl (Cooper et al., 1997). GAPDH exerts also a role in neurodegenerative diseases characterized by the expansion of CAG repeats, resulting in inhibition of GAPDH activity and in protein-protein interaction of GAPDH with huntingtin and atrophin (Burke et al., 1996), ataxin (Koshy et al., 1996), the androgen receptor or the β-amyloid precursor protein (Schulze et al., 1993).

We recently described a trans-plasma membrane NADH-dichlorophenol-indophenol oxidoreductase (PMO) in neuronal plasma membrane (Yong and Dreyer, 1995; Zurbriggen and Dreyer, 1996). The activity of the purified enzyme (from bovine or rat brain and neuroblastomas) could be attributed to a tight complex consisting of five components: GAPDH,

Hsc70, Ulip2, enolase-γ (brain specific) and aldolase C (brain specific zebrin II) (Bulliard et al., 1997). These components are also essential factors in various neurodegenerative diseases. PMOs play a central function in mediating cellular responses against oxidative stress (Dastoor and Dreyer, 2000) and have a high impact on major cellular processes. However the molecular mechanisms and cellular dynamics that underlie these processes or the interactions of the members of the multi-protein complex, and the function and biological relevance of this complex are unknown. To clarify these, we have investigated the cellular distribution of GAPDH, the major component of the PMO complex, after induction of oxidative stress or apoptosis. By means of confocal laser-scanning microscopy and immunocytochemistry, we studied the subcellular distribution of endogenous GAPDH and the effects of transient and stable overexpression of GAPDH-GFP in either central nervous system (CNS)-derived cells (mouse neuroblastoma NB41A3), non-CNS derived cells (R6 fibroblast) or an apoptosis-resistant Bcl2-expressing R6 cell line (R6-Bcl2).

MATERIALS AND METHODS

Cell culture

Neuroblastoma cells NB41A3 were obtained from ATCC (Bethesda, MD) and maintained as monolayers on tissue culture plastic flasks at 37°C in a humidified atmosphere of 5% CO_2/95% air, as previously described (Augusti-Tocco and Sato, 1969). The growth medium was Dulbecco's modification of Eagle's medium (DMEM) at pH 7.4, containing 3.7 g/l $NaHCO_3$, 4.5 g/l D-glucose, 0.11 g/l sodium pyruvate and 0.58 g/l glutamine, 10% fetal calf serum (FCS), 50 units/l of penicillin and 50 μg/l of streptomycin. The rat 6 embryo fibroblast cell line (R6) and a derivative that stably overexpresses Bcl2 (R6-Bcl2) were kindly provided by Dr C. Borner (Institute of Biochemistry, Fribourg, Switzerland; Borner, 1996). They were grown in the same way as the neuroblastoma cells, except that the culture medium contained 5% instead of 10% FCS.

For all cell lines, the medium was changed every 3 days. Starving of the cultures and growth to post confluence were strictly avoided. The cells were trypsinized in the presence of 0.25% trypsin and 0.1% EDTA (for splitting) or harvested (for RNA or protein extracts) when they were subconfluent.

Construction of plasmids

The complete coding region of GAPDH was amplified as two overlapping pieces by RACE from mouse brain Marathon cDNA (CLONTECH). The 3′-end and the overlapping 5′ end were created with an adapter primer (CCATCCTAATACGACTCACTATAGGGC), and the GAPDH-specific downstream (TTG GCA GGT TTC TCC AGG CGG CAC) or upstream primer (CTC ACG GCA AAT TCA ACG GAC CAG). The amplified products were subcloned into the pKS+ Bluescript (Stratagene, La Jolla, CA) and the sequence confirmed by sequencing. Subsequently, the amplified DNA sequence was cut out of pKS+ Bluescript and subcloned in-frame with the green fluorescent protein (GFP)-coding sequence in pEGFP-N1 or pEBFP-N1 (both Clontech), respectively.

The 5′-RACE and the 3′-RACE fragments were joined at their common *Nsi*I restriction site in the overlapping sequence. The 3′-end of this GAPDH construct was ligated at a *Sfi*I restriction site to an adapter (5′-TGG CCT CCA AGG AGG GGG GTG GTAC-3′ and 3′-TGT ACC GGA GGT TCC TCC CCC CAC CAT GGG CC-5′) that replaced the stop codon of GAPDH by nucleotides coding for three glycine residues. This whole construct was ligated in frame into pEGFP or pEBFP expression vector at the *Xma*I restriction site. Control plasmids that do not produce the GFP, only the GAPDH protein, were prepared by disrupting the GFP sequence by a frameshift mutation at the artificial *Kpn*I/*Asp*718 restriction site between the 3′-end of the GAPDH gene and the start codon of GFP. Correct expression of these constructs was confirmed by immunofluorescence assays in transfected cells. All plasmids were purified on QIAGEN Midi columns.

Transfection

Cells grown on 12 mm glass coverslips in six-well plates were transfected at 80-90% confluence using SuperFect (Qiagen). 1 μg of plasmid DNA suspended in 60 μl fresh DMEM without serum and 5 μl SuperFect were mixed, vortexed and incubated for 10 minutes, before adding 600 μl of complete growth medium. The mixture was then immediately transferred to PBS-washed cells. After 3-4 hours of incubation at 37°C/5% CO_2, cells were washed once with PBS.

To produce stable NB41A3 cell lines that overexpress GAPDH-GFP, NB41A3 cells plated on tissue culture plastic were transfected and split 2 days later in medium containing 0.75 mg/ml G418 (Life Technologies). Selection medium was changed every 3 days for a period of 3 weeks, after which G418-resistant colonies were selected and analyzed under the microscope for GFP expression.

Induction of oxidative stress and apoptosis

Immediately after transient transfection, cells were trypsinized, split 1:3 and plated on glass coverslips placed in six-well plates. After 24 hours the growth medium was replaced by new medium (control) or new medium containing either 300 μM FeCN, 100 μM H_2O_2, 1.5 μM MG132 or 200 nM staurosporine. Cells were exposed for 3 hours (to 300 μM FeCN or 100 μM H_2O_2) and for 6 hours or 24 hours (to 200 nM staurosporine or 1.5 μM MG132) and then analyzed under the microscope.

Immunocytochemistry

The following primary antibodies were used: mouse anti-GAPDH Mab (IgG) (ANAWA), rabbit anti-NSEγ polyclonal antibody (Chemicon International), mouse anti-aldolase C Mab (IgG) (obtained through the courtesy of Dr R. Hawkes, University of Calgary, Calgary, Alberta, Canada) and rabbit anti-GFP polyclonal antibody (IgG) (Clontech Laboratories, Palo Alto, CA). As secondary antibodies Texas Red-conjugated goat anti-mouse IgG, Texas Red-conjugated goat anti-rabbit IgG, fluorescein isothiocyanate (FITC)-conjugated goat anti-mouse IgG or FITC-conjugated goat anti-rabbit IgG (Jackson ImmunoResearch Laboratories, Bar Harbor, ME) were used for immunocytochemistry.

When native GFP fluorescence was used to localize the GFP fusion proteins, the coverslip containing the adherent cells was directly placed on top of a drop of growth medium without Phenol Red on a microscope slide and immediately analyzed.

Otherwise, cells were rinsed twice in PBS and fixed for 15 minutes in 4% paraformaldehyde in 0.1 M Pipes (pH 6.8) containing 0.1% Hoechst 33342. Cells were then rinsed twice in PBS, permeabilized for 5 minutes with 0.05% saponin in Pipes, again rinsed twice in PBS and incubated for 10 minutes at –20° C in acetone. After two washes with PBS, cells on the coverslip were incubated in 1% BSA in PBS for 2 hours with the first antibody, rinsed twice in PBS and further incubated for 2 hours with the fluorescent secondary anti-IgG before two washes in PBS. Fluorescence was extended by using SlowFade (Molecular Probes, Leiden, Netherlands). All incubations were performed in a light-protected environment and (except for those involving acetone) at room temperature.

Fluorescence microscopy

Cells were examined with a Nikon Eclipse E800 microscope under a 100× oil immersion objective (Nikon) using a MRC-1024 BioRad laser confocal microscope system equipped with an Krypton/Argon laser (BioRad Labs, Hercules, CA) and the LaserSharp acquisition

software (BioRad). Serial sections (at 0.5-1.5 μm intervals) in the *z*-axis of cells were collected in the slow scanning mode (~160 Hz) with 1.5-4.5 mm diameter iris aperture by averaging pictures by Kalman (3 scan). Monochrome densities were collected with high-density precision at 12 bit resolution. Green fluorescence (GFP or FITC) and Texas Red were detected in parallel at 512×512 pixels. The pictures were processed with the LaserSharp processing software (BioRad) or with ConfocalAssistant before picture files were transferred to Adobe Photoshop 4.0 and printed on a Kodak printer. To visualize DNA staining with Hoechst 33342, a 100× oil immersion Plan-Neofluar objective (Zeiss) with an inverted Zeiss Axiovert 135 TV microscope equipped with a HBO 100-XBO 75 lamp was used.

Quantification

The serial sections through the *z*-axis of the cell were collected within a linear range of fluorescence intensity, superimposed to a 3D stack and analyzed as a 2D projection. To compare GFP expression in different subcellular structures, the mean pixel intensity in the whole cell (cytoplasm, organelles and nucleus) was determined and normalized after subtracting the background, which yielded an integrated density of 100%. In short, all sections collected in the *z*-axis of the appropriate picture by laser-scanning confocal microscopy are stacked to a two-dimensional projection in which the intensities of the various sections are accumulated. A plot (pixel intensity versus pixel counts) is then prepared from the area under investigation in the 2D-projection, evaluating the mean pixel intensity and the distribution of pixel intensities versus the s.d. A high mean pixel intensity correlates to high amount of expressed protein, whereas a high s.d. indicates a patchy, irregular expression in the specific area. From this analysis the ratio of cytoplasmic to nuclear localization can be accurately quantified. Ratios over 1.0 display predominantly cytoplasmic localization. Each experiment consisted of analyzing 15 cells and was repeated three times. Thus, each data point in Fig. 3 and in the tables indicates the average of 45 individual measurements from three individual analyses of different populations. In our optimized conditions, quantification is reproducible and the ratios measured between cytoplasmic and nuclear GAPDH are appropriate within ~3-4% s.d. Changes in translocation by 5% are statistically significant at $P<0.1$.

RESULTS

Untransfected cells expressing endogenous GAPDH

Cell-specific subcellular localization of endogenous GAPDH in the absence of apoptotic stimuli or oxidative stress

The distribution of endogenous GAPDH in NB41A3 cells (a CNS-derived cell line) was about equally distributed in the cytoplasm and in the nucleus (Fig. 1A,B). In contrast in R6 fibroblast cells and R6-Bcl2 cells, an apoptosis-resistant Bcl2-expressing cell line, most endogenous GAPDH (80%) is localized in the cytoplasm (Fig. 1A). Unstressed NB41A3, R6 or R6-Bcl2 cells showed no signs of apoptosis (Table 1).

Nuclear translocation of endogenous GAPDH induced by oxidative stress

After oxidative stress with 100 μM H_2O_2, 75% of GAPDH was localized in the nucleus in NB41A3 cells (Fig. 1A,B). In both R6 or R6-Bcl2 cells, translocation of GAPDH to the nucleus increased by about 30% (Fig. 1A,D). R6 did not display a uniform distribution of GAPDH in the nucleus or in the cytoplasm, but higher concentrations of GAPDH were found around the nucleolus. A ‘speckled’ pattern for GAPDH, associated with cell-surface blebbing, was seen sometimes in NB41A3 cells (Fig. 1C). In both, R6 and R6-Bcl2 cells, GAPDH also accumulated in intracellular clusters, similar to speckles (Fig. 1C,D). The ratio of nuclear translocation and speckles formation in response to oxidative stress is unchanged by Bcl2. Oxidative stress did not induce apoptosis. Similar results were observed when oxidative stress was induced with 300 μM FeCN (data not shown).

Nuclear translocation of endogenous GAPDH after induction of apoptosis by staurosporine and MG132

Staurosporine caused nuclear translocation of endogenous GAPDH. As shown above, endogenous GAPDH is initially mainly cytoplasmic in R6 cells (Fig. 2A). After exposure to 200 nM staurosporine for 6 hours, an accumulation of GAPDH in the nucleus in R6 cells (Fig. 2A) and an increase from 55% to more than 65% of nuclear GAPDH in NB41A3 cells (Fig. 1B) is observed. Cells that show apoptotic features (such as nuclear fragmentation) were very rare. The apoptotic cells were small, shriveled up and round. The number of apoptotic cells (Fig. 2A) is further increased after 24 hours exposure to staurosporine. In most non-apoptotic cells, GAPDH levels increased by only about 50%, whereas in apoptotic cells GAPDH expression increased up to 300% (Table 2), but was excluded from the fragmented DNA. At a later stage, however, some apoptotic cells become depleted of GAPDH (Fig. 2A).

MG132 had effects very similar to staurosporine (Table 1). Similarly, in NB41A3 an increase of nuclear GAPDH was observed after 6 hours and 24 hours exposure to apoptotic agents (Fig. 1B). Some NB41A3 cells changed to a ‘hedgehog’-like morphology (spiked), other NB41A3 cells were round and formed blebs containing GAPDH, but did not show nuclear fragmentation (Fig. 2B). Like apoptotic fibroblasts, apoptotic NB41A3 cells also accumulated very high levels of GAPDH.

Bcl2 prevents nuclear translocation of endogenous GAPDH and makes cells more resistant to apoptosis induced by staurosporine and MG132

After exposure to 200 nM staurosporine for 6 hours, 5% of NB41A3 cells and 10% of R6 cells are apoptotic (Table 1).

Table 1. Apoptosis in untransfected and GAPDH-GFP transfected cells

	Apoptotic cells*				
		MG132		Staurosporine	
	Control	6 hours	24 hours	6 hours	24 hours
	%	%	%	%	%
NB41A3 unstransfected	0	2	20	5	20
NB41A3 transiently transfected	10	15	35	20	40
NB41A3-GAPDH-GFP	5	15	35	15	35
R6 untransfected	0	10	70	10	50
R6 transfected	10	55	90	70	85
R6-Bcl2 untransfected	0	2	20	5	15
R6-Bcl2 transfected	10	45	85	60	90

*The percentages of apoptotic cells after 6 hours and 24 hours of incubation with either MG132 (1.5 μM) or staurosporine (200 nM) are indicated. Cells showing chromatin condensation or nuclear fragmentation, which was visualized by Hoechst Blue staining, were considered as apoptotic cells. s.d. is less than 5% ($P<0.1$) in all tested conditions.

After 24 hours, the number of apoptotic cells increases to about 20% for NB41A3 cells and to 50% for R6 cells. Under similar experimental conditions, only 5% of R6-Bcl2 cells are apoptotic after 6 hours, increasing to 15% after 24 hours, significantly less than R6 cells, because Bcl2 protects cells from apoptosis (Table 1). Observations were similar after induction of apoptosis by MG132 (Table 1).

Under similar conditions, apoptotic features were found in only 2% of R6-Bcl2 cells after 6 hours and in 20% cells after 24 hours (Table 1), consistent with the fact that Bcl2 protects cells from apoptosis. In addition, Bcl2 decreased the amount of nuclear translocation of endogenous GAPDH after exposure to either staurosporine or MG132. Most cells still display GAPDH predominantly in the perinuclear area and cells with higher amounts of nuclear translocation had fewer processes.

Effects of overexpression of GAPDH-GFP

GFP-tag does not influence cell viability and subcellular localization of transfected GAPDH-GFP

Overexpression of GAPDH was generated by transfecting either GAPDH or a GAPDH-GFP hybrid. Under our experimental conditions, transfection efficiency is about 15% in all cell lines. Transfection of GFP alone as a control showed that in NB41A3 cells (Fig. 3A) as well as in R6 cells (Fig. 3A) GFP was uniformly expressed all over the cell. No nuclear fragmentation was observed and, independent of the level of GFP expression, no differences in morphology or cell viability

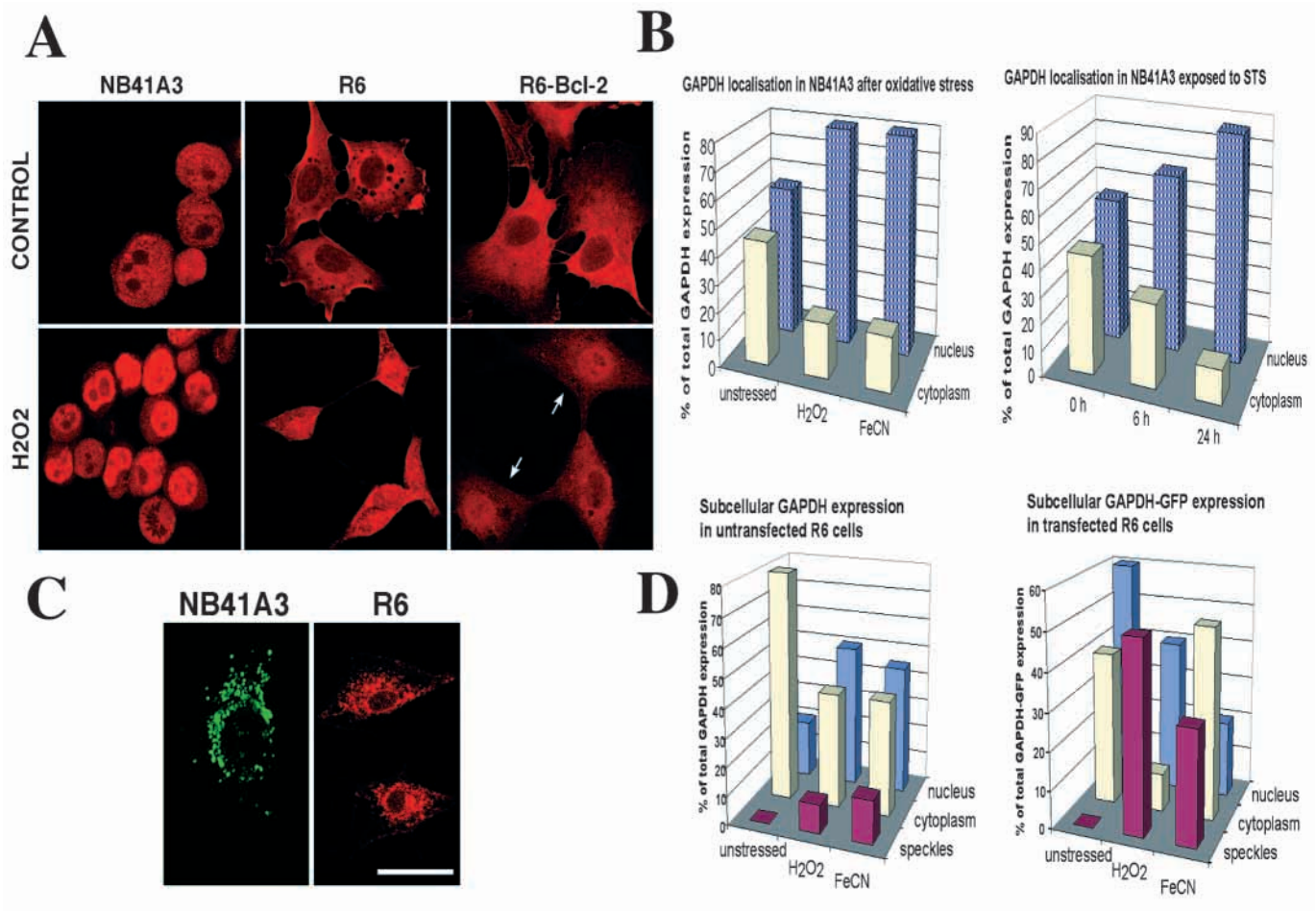

Fig. 1. Subcellular localization of endogenous GAPDH in untransfected cells under unstressed conditions or after induction of oxidative stress. (A, top) Localization in unstressed cells. Nuclear localization of endogenous GAPDH in NB41A3 cells, R6 or R6-Bcl2 cells. Detection of GAPDH by Texas Red. (A, bottom) Induction of oxidative stress by exposure to 100 μM H_2O_2 for 3 hours. Nuclear translocation of endogenous GAPDH (detected by Texas Red immunocytochemistry) in NB41A3, R6 and R6-Bcl2 cells. Detection of GAPDH by Texas Red. Arrows indicate cells with nuclear localization of GAPDH. (B) Subcellular localization of GAPDH in NB41A3 cells after oxidative stress and induction of apoptosis. (Left) Untransfected NB41A3 cells were analyzed under unstressed conditions or after 3 hours of oxidative stress with either 100 μM H_2O_2 or 300 μM FeCN. Oxidative stress induces nuclear translocation of GAPDH in untransfected cells. (Right) Untransfected NB41A3 cells were treated with 200 nM staurosporine (right) were analyzed. The percentage of total endogenous GAPDH in the nucleus and in the cytoplasm is indicated. Increase of nuclear translocation of GAPDH correlates with longer exposure times to staurosporine. (C) Accumulation of GAPDH in speckles in NB41A3 (left) and R6-Bcl2 cells (right). Detection of GAPDH by Texas Red (right) or FITC staining of anti-GAPDH antibody (left). (D) Subcellular expression of GAPDH in untransfected (left) and transiently transfected R6 cells (right). Cells were analyzed under unstressed conditions or after 6 hours of oxidative stress with either 100 μM H_2O_2 or 300 μM FeCN. The percentage of total GAPDH (or of GAPDH-GFP for transfected cells) in the nucleus, in the cytoplasm or in speckles is indicated. Nuclear expression of GAPDH and formation of speckles is higher in GAPDH-GFP transfected cells. Nuclear translocation of GAPDH is induced by H_2O_2. Scale bar in C: 50 μm.

were observed compared with untransfected cells (data not shown). Induction of oxidative stress with 100 μM H_2O_2 for 3 hours did not change the cell morphology or the distribution of GFP. After exposure to pro-apoptotic reagents, the percentages of GFP-transfected apoptotic NB41A3 and R6 cells were comparable with untransfected cells (data not shown). Cells were shriveled up and showed slightly increased levels of GFP; however, there was no increased nuclear translocation of GFP.

The effect of the GFP-tag on protein localization was tested by transfection with either the GAPDH-GFP or the GAPDH (without tag) expression vector. The subcellular distribution of transfected GAPDH (red) was similar to that of transfected GAPDH-GFP (green) irrespective of whether cells were unstressed or stressed with H_2O_2 (Fig. 3B). In addition, the number of cells undergoing apoptosis in response to staurosporine or MG132 were comparable. These observations indicate that the GFP tag does not influence the expression pattern and the cellular localization of GAPDH. The anti-GAPDH antibodies detect the GAPDH-GFP, and both the green fluorescence (from GFP) and the red fluorescence (from Texas Red-anti-GAPDH antibodies) co-localize fully (also after oxidative stress induced by H_2O_2, and induction of apoptosis; see Fig. 5H,K). These antibodies also detected endogenous GAPDH in non-transfected cells.

Transfected cells have increased nuclear localization of GAPDH-GFP

In contrast to untransfected cells, in transiently transfected NB41A3 cells, most GAPDH-GFP (75%) was concentrated in the nucleus under basal conditions (Fig. 3B,C). Similar results were observed in a NB41A3-derived cell line, which stably overexpresses GAPDH-GFP (NB41A3-GAPDH-GFP) (Fig. 3C).

In R6 and in R6-Bcl2 cells the localization of transiently transfected GAPDH-GFP was quite similar in both cases. 30% of either R6 or R6-Bcl2 cells displayed GAPDH-GFP predominantly in the cytoplasm, similar to untransfected cells. In the remaining 70% of cells, GAPDH-GFP localization was predominantly nuclear after transfection (Fig. 1D). The percentage of nuclear localization in transfected R6 cells was thus smaller than in transfected NB41A3 neuroblastomas.

Apoptosis is observed after overexpression of GAPDH-GFP and is not inhibited by Bcl2

As shown above, in spite of the predominantly nuclear localization of GAPDH, most of the cells overexpressing GAPDH-GFP are not apoptotic. However, under resting conditions nuclear fragmentation was seen in 10% of NB41A3 cells that overexpressed GAPDH-GFP (Table 1). These apoptotic cells expressed higher levels of GAPDH-GFP than non-apoptotic cells (Fig. 4A, Table 2). In transfected R6 fibroblasts, the number of apoptotic GAPDH-GFP is also about 10%, irrespective of whether they overexpress Bcl2 or not (Table 1). These cells were shriveled up and displayed two- to threefold higher levels of GAPDH-GFP around the segmented DNA (Fig. 4A).

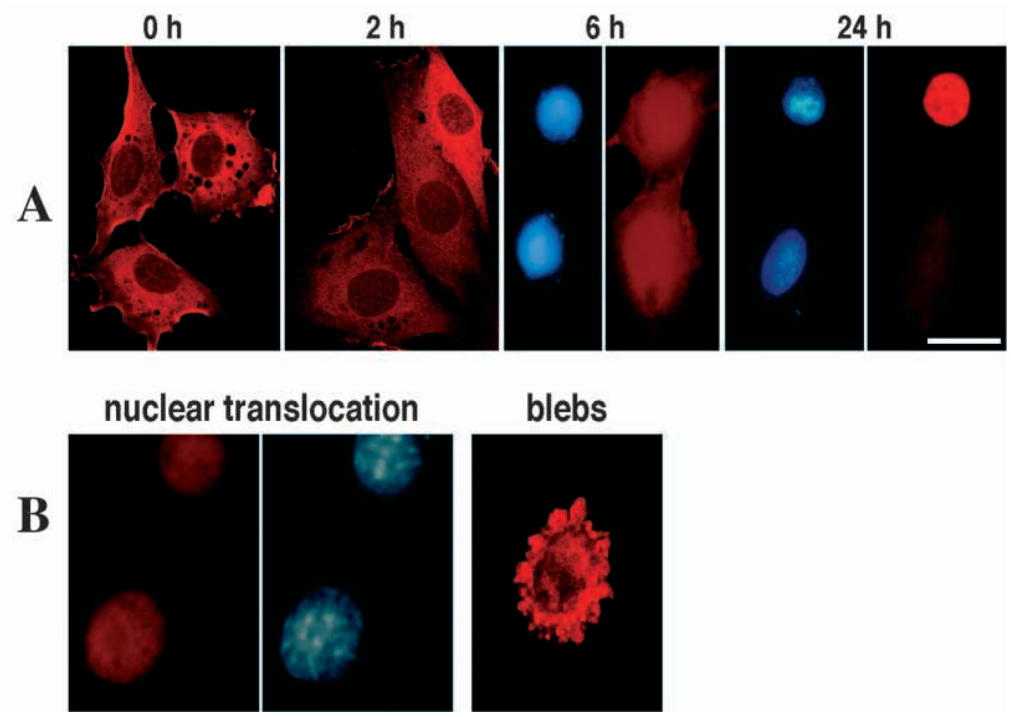

Fig. 2. Subcellular localization of endogenous GAPDH in untransfected cells after induction of apoptosis. (A) Subcellular localization in R6 fibroblast cells: From left to right, R6 cells treated with 200 nM staurosporine for 0 hours, 2 hours, 6 hours or 24 hours. Subcellular localization of GAPDH is unchanged after 2 hours, but increased nuclear expression is already observed after 6 hours. Visualization of DNA by Hoechst Blue staining and detection of GAPDH by Texas Red staining of anti-GAPDH antibody. (B) Nuclear translocation (left) and bleb-formation (right) in NB41A3 cells after induction of apoptosis for 6 hours with 1.5 μM MG132. Detection of GAPDH by Texas Red staining of anti-GAPDH antibody or by Hoechst Blue staining for visualization of DNA. Scale bar in A: 50 μm.

Nuclear translocation of GAPDH-GFP is observed after induction of oxidative stress by H2O2

Exposure to H_2O_2 enhanced nuclear translocation of GAPDH-GFP in transfected NB41A3 cell lines (Fig. 3B). After 3 hours of oxidative stress induced by 100 μM H_2O_2 the nuclear GAPDH-GFP levels rose from 70% to nearly 90% (Fig. 3C). No expression was observed in the nucleolus.

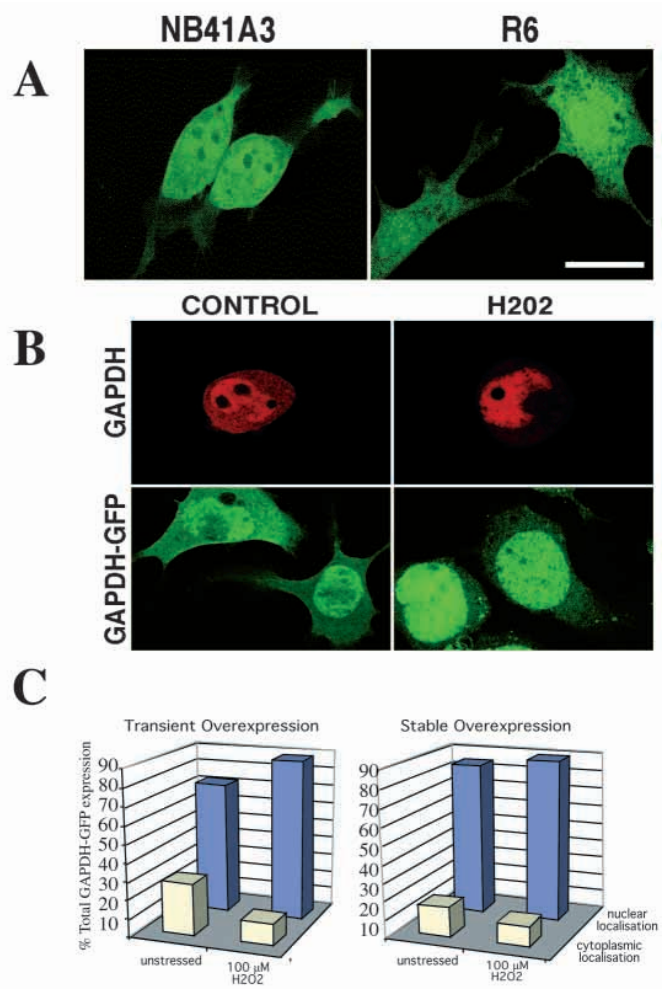

Fig. 3. Cellular localization of GAPDH-GFP in transiently or stably transfected NB41A3, R6 cells and R6-Bcl2 cells. (A) Controls of transfection with pEGFP: cellular localization of GFP in NB41A3 neuroblastoma cells (left) or in R6 fibroblast cells (right) transfected with pEGFP, a control vector devoid of GADPH gene. GFP is expressed in the entire cell. Viability of the cells was not influenced by transfection with GFP. (B) NB41A3 cells stably transfected with pGAPDH, a vector devoid of GFP-tag (top), or stably transfected with GAPDH-GFP (bottom). The expression of GAPDH as detected by Texas Red immunocytochemistry (top) or as GFP fluorescence (bottom) was tested in unstressed NB41A3 cells and in NB41A3 cells stressed with 100 μM H_2O_2. Under similar conditions the expression is similar in both cell types. (C) Subcellular localization of GAPDH after oxidative stress and induction of apoptosis. NB41A3 cells transiently transfected with GAPDH-GFP (left) and NB41A3 cells stably transfected with GAPDH-GFP (right) were analyzed under unstressed conditions or after 3 hours of oxidative stress with 100 μM H_2O_2 The percentage of total GAPDH (or of GAPDH-GFP for transfected cells) in the nucleus or in the cytoplasm is indicated. Oxidative stress by H_2O_2 induces nuclear translocation of GAPDH. Each experiment consisted of analyzing 15 cells and was repeated three times. Thus, each data point indicates the average of 45 individual measurements. s.d. is smaller than 5% in all tested conditions.

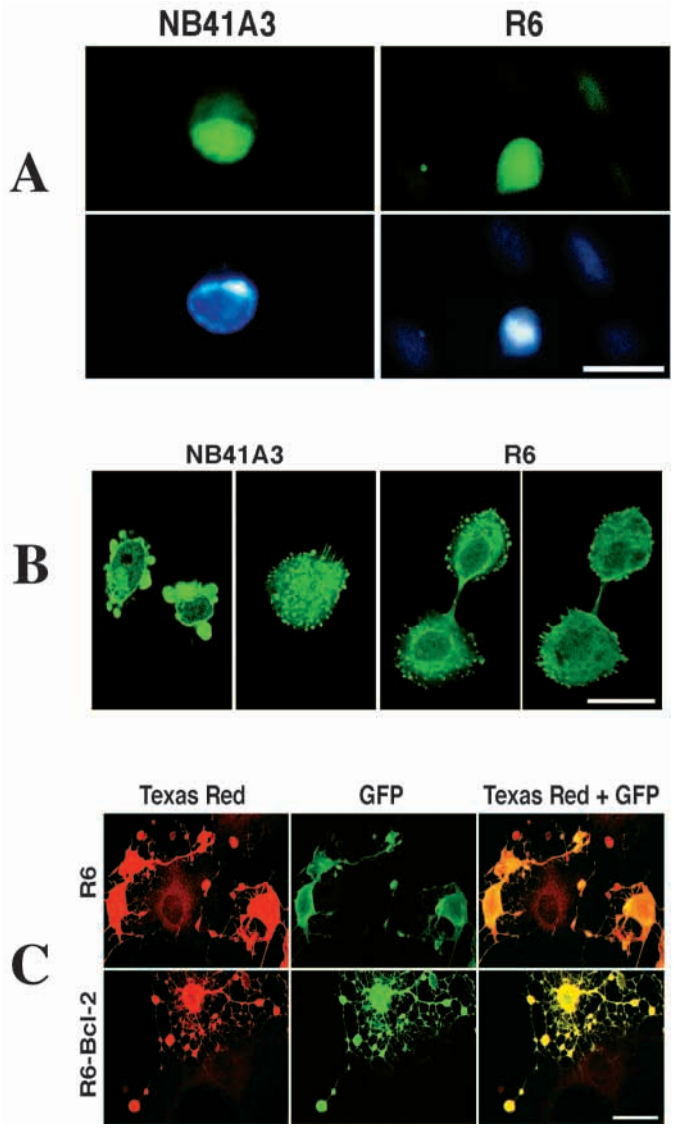

Fig. 4. Subcellular translocation and induction of apoptosis, blebs and processes in overexpressing cells. (A) Unstressed cells transfected with GAPDH-GFP. Nuclear expression of GAPDH-GFP in transiently transfected NB41A3 neuroblastoma cells (left) or in R6 fibroblasts (right). Transient overexpression of GAPDH-GFP leads to 10% apoptotic cells, detected by Hoechst staining (bottom) or as GFP fluorescence (top). (B) Morphological changes after exposure to apoptotic agents. From left to right, respectively, formation of GAPDH-GFP blebs in transiently transfected NB41A3 cells after oxidative stress; 'hedgehog'-like NB41A3 cell after exposure to 1.5 μM MG132 for 6 hours; two subsequent confocal planes of two adjacent 'hedgehog'-like R6 cells forming speckles and spikes attached to the cell surface after exposure to 1.5 μM MG132 for 6 hours. (C) Formation of long processes and high expression of GAPDH-GFP in transfected (top) R6 and (bottom) R6-Bcl2 cells (but not in untransfected cells), after exposure to 200 nM staurosporine for 6 hours. Texas Red staining by anti-GAPDH (left), GAPDH-GFP fluorescence (center), and overlay of GFP and Texas Red fluorescence (right). Visualization of transfected GAPDH by GFP fluorescence from the GFP tag. Scale bars: 50 μm.

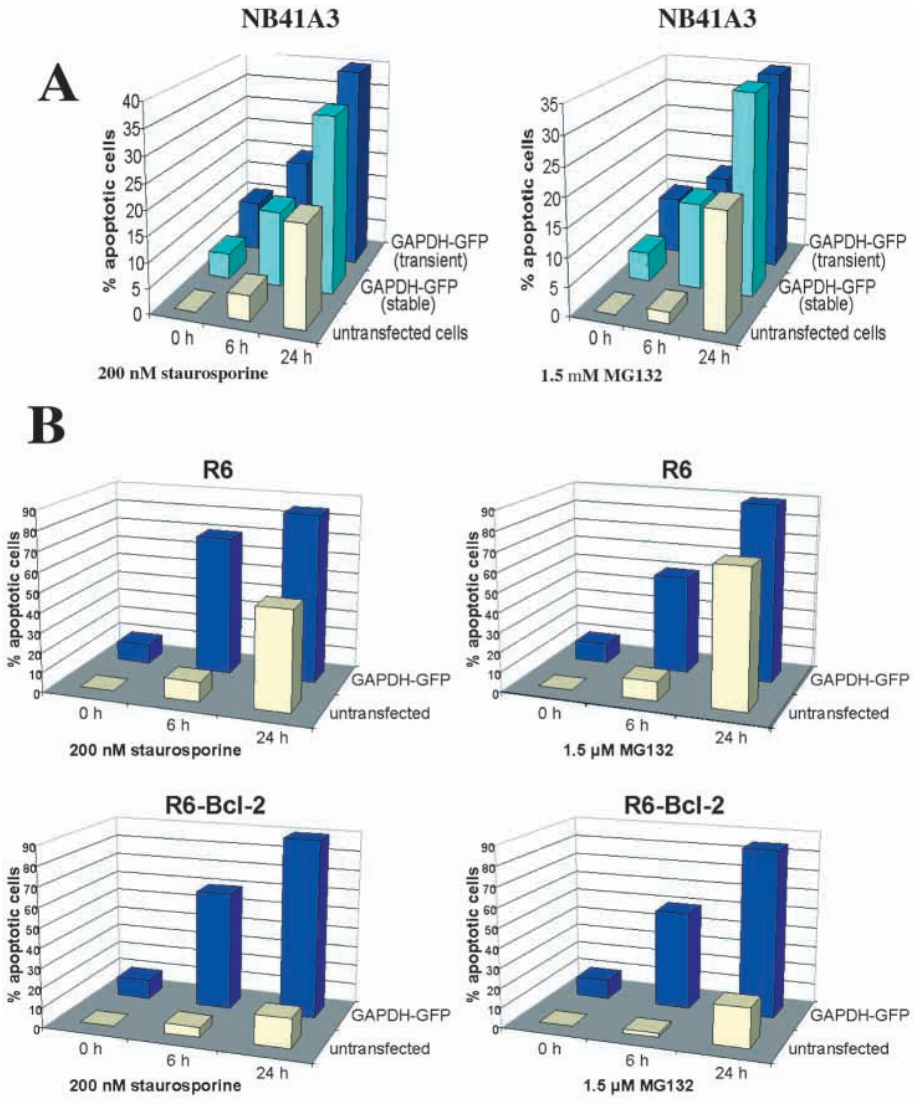

Fig. 5. Apoptosis after exposure of cells to staurosporine and MG132. Percentage of apoptosis in NB41A3 cells untransfected, transiently transfected and stably transfected with GAPDH-GFP and treated with 200 nM staurosporine (left) or 1.5 μM MG132 (right). Transfected NB41A3 cells are more sensitive to induction of apoptosis by staurosporine or MG132 than untransfected cells. (B) R6 cells (top) or R6-Bcl2 cells (bottom) were exposed to 200nM staurosporine (left) or 1.5 μM MG132 (right). Untransfected fibroblasts are less sensitive to induction of apoptosis by staurosporine or MG132. Overexpression of Bcl2 can protect untransfected but not GAPDH-GFP transfected cells from apoptosis. Induction of apoptosis by staurosporine (200 nM) or MG132 (1.5 μM) was performed as described. The percentage of cells showing nuclear fragmentation or chromatin condensation in cells expressing endogenous GAPDH or transfected GAPDH-GFP is indicated after 0, 6 and 24 hours of exposure time. Each data point is an average of three individual populations, each containing at least 50 cells. s.d. is less than 5% in all tested conditions.

Exposure of R6 and R6-Bcl2 cells to H_2O_2 induced drastic changes in GAPDH-GFP localization within 3 hours (Fig. 1D). GAPDH-GFP mostly accumulated in the nucleus and displayed a punctuated expression pattern, sometimes arranged in intracellular speckles, much more frequently observed than in untransfected fibroblasts. NB41A3, R6 and R6-Bcl2 cells with very high expression levels of GAPDH-GFP formed GAPDH-GFP-positive intracellular speckles. Increased translocation of GAPDH-GFP and the formation of GAPDH-positive speckles correlated with increasing concentrations of stress agents and longer exposure time (data not shown). Oxidative stress induced by 100 μM H_2O_2 did not increase the percentage of nuclear fragmentation in GAPDH-GFP-overexpressing cells. However, in few cells, and exclusively after stress, overexpression of GAPDH-GFP at very high levels (associated with pronounced blebbing of the cell surface membrane), was observed. Bcl2 did not influence the response to oxidative stress.

In GAPDH-GFP transfected cells, changes in cell morphology, nuclear translocation of GAPDH-GFP, which is observed after exposure to apoptotic agents, cannot be prevented by Bcl2

Apoptotic agents changed both the cell morphology and the localization GAPDH. After 6 hours of incubation with either staurosporine or MG132, in contrast to untransfected cells, many NB41A3 cells, either transiently or permanently overexpressing GAPDH-GFP, changed their morphology. Most cells have increased nuclear levels of GAPDH-GFP (about 50% more than control cells) and displayed long axons that form a network-like structure (similar to Fig. 4C). These non-apoptotic NB41A3 cells express GAPDH distributed equally between the nucleus and the cytoplasm. The number of 'hedgehog'-like spiked NB41A3 cells (Fig. 4B) (all displaying an unfragmented nucleus) increased nearly twofold compared with untransfected cells. In a few cells, GAPDH-GFP was associated with cell surface blebs (Fig. 4B). Apoptotic NB41A3 cells are much smaller and shriveled up and have fragmented nuclei. They express GAPDH-GFP at very high levels: three times higher than basal levels (Table 2).

Staurosporine had similar effects on both R6 or R6-Bcl2 cells; in particular nuclear translocation of GAPDH-GFP was not prevented by Bcl2. Non-apoptotic cells often either showed nuclear translocation of GAPDH-GFP or formed a network of interconnected long processes, which contained junctions where the processes formed enlarged knots (Fig. 4C). The whole network including the knots and the main cell body expressed 2-3-fold more GAPDH-GFP compared with controls, but no nuclear fragmentation was detected. Some R6

Table 2. Relative mean pixel intensity of total GAPDH expression in NB41A3 cells

		Relative mean pixel intensity*		
		Untreated	MG132	Staurosporine
		%	%	%
Endogenous GAPDH	Non-apoptotic cells	100	100	100
	Apoptotic cells	-	280	280
Transfected GAPDH-GFP	Non-apoptotic cells	250	250	250
	Apoptotic cells	600	600	600

*The relative mean pixel intensity was obtained by measuring total GAPDH expression and mean pixel intensity in several apoptotic and non-apoptotic cells. The mean intensity of endogenous GAPDH in non-apoptotic cells was defined as 100%. Apoptosis was induced by incubation with either 200 nM staurosporine or 1.5 μM MG132 for 24 hours.

cells also had a 'hedgehog'-like shape and showed a speckled pattern of GAPDH-GFP expression or blebs (Fig. 5D,E).

GAPDH-GFP transfected cells are more sensitive to apoptosis and, in contrast to cells expressing only endogenous GAPDH, cannot be protected from apoptosis by overexpression of Bcl2

After 6 hours and 24 hours exposure to staurosporine 15-20% and 35-40% (respectively) of NB41A3 cells with overexpressed GAPDH-GFP (transiently or permanently) had fragmented nuclei, twice more than the number in untransfected cells (Fig. 5A). Similarly, R6 cells transfected by GAPDH-GFP are also more sensitive to apoptosis induced by staurosporine than untransfected ones: after 6 hours and 24 hours of exposure about 70% and 85% of the cells (respectively) showed signs of apoptosis (Fig. 5B). The percentages of apoptotic GAPDH-GFP transfected R6-Bcl2 cells were very similar (60% and 90%, respectively, Table 1), indicating that Bcl2 is able to prevent apoptosis in untransfected cells, but not in transfected cells that overexpress GAPDH-GFP.

During apoptosis induced by MG132, after 6 hours and 24 hours 15% and 35% (respectively) of GAPDH-GFP transfected neuroblastoma cells were apoptotic (Fig. 5A). Under similar conditions 45% and 85% of the GAPDH-GFP transfected R6 cells (respectively) were apoptotic (Fig. 5B). This showed that NB41A3 and R6 cells that overexpressed GAPDH-GFP are more sensitive to MG132 than untransfected cells. In these experiments, overexpression of Bcl2 in GAPDH-GFP transfected R6 cells also failed to decrease the number of apoptotic cells (Fig. 5B).

Overexpression of other proteins of the neuronal PMO complex can modulate the expression of GAPDH

In order to test whether components of the PMO complex (enolase, Ulip, Hsc70 and aldolase) influence GAPDH-GFP translocation, BFP-tagged genes were prepared and co-transfected. Co-transfection of Ulip-GFP or enolase-BFP with GAPDH-GFP did influence the amount of nuclear translocation of GAPDH in NB41A3 cells after oxidative stress.

Concomitant overexpression of GAPDH with either aldolase or Hsc70, both of which are present predominantly in the cytoplasm, increased cytoplasmic distribution of GAPDH in both unstressed and stressed cells. Prior to oxidative stress, 52 and 55% of GAPDH was localized in the cytoplasmin cells co-transfected with aldolase and Hsc70, respectively, and after stress with 100 μM H_2O_2, 40% of this GAPDH remained in the cytoplasm (compared with 28% before stress and 12% and after stress, in cells transfected with GAPDH alone). These observations indicate that overexpression of Hsc70 or aldolase, two components of the neuronal PMO complex, partially prevents nuclear translocation of GAPDH (Table 3) (for more details, see Dastoor and Dreyer, 2000).

Together these data indicate that the components of the neuronal PMO complex modulate the intracellular translocation of GAPDH during oxidative stress.

DISCUSSION

Very accurate quantitative measurements by means of confocal laser-scanning microscopy have been achieved to assess the cellular localization of GADPH under different experimental conditions, much more accurate than those obtained by biochemical methods based on cell fractionation. In the optimized conditions developed in this study, our procedures are highly reproducible and the ratios measured between cytoplasmic and nuclear GAPDH are appropriate within ~3-4% s.d. Confocal microscopy also enables the specific observation and analysis of statistically significant changes in the cells transfected with GAPDH-GFP, even if these changes are relatively small, about 15%, compared with a high background from endogenous GAPDH. Other methods cannot monitor such small changes or distinguish endogenous from overexpressed protein.

Nuclear localization of GAPDH is not sufficient to induce apoptosis per se

The major action of GAPDH takes place in the cytoplasm during glycolysis. Exclusive or at least highly predominant cytoplasmic localization of GAPDH, has been described in COS-7 cells (Tajima et al., 1999), S49 cells, primary thymocytes (Sawa et al., 1997), PC12 cells, HEK 293 cells, COS-1 cells (Sawa et al., 1997; Shashidharan et al., 1999), epithelial cells (Epner et al., 1999) and cultured CGCs (Ishitani et al., 1998; Saunders et al., 1997; Saunders et al., 1999). Consistent with these studies, we have found that resting R6 fibroblasts, in which apoptosis is not induced, display endogenous GAPDH predominantly in the cytoplasm.

Table 3. Influence of co-transfection of other components from the neuronal PMO complex on expression of GAPDH-GFP

Protein co-expressed with GAPDH-GFP	GAPDH-GFP localization in the nucleus*	
	Control	H_2O_2
	%	%
GAPDH-GFP only	72	88
Enolase-BFP	70	85
Ulip-BFP	70	90
Aldolase-BFP	48	60
Hsc70-BFP	45	60

*The percentages of cells accumulating GAPDH-GFP in intracellular speckles and the percentage of GAPDH-GFP expressed in the nucleus are indicated for transiently transfected cells, which were analyzed under unstressed conditions or after 6 hours of oxidative stress with either 100 μM H_2O_2 or 300 μM FeCN. s.d. is less than 5% ($P<0.1$) in all tested conditions.

However, in unstressed NB41A3 neuroblastoma cells, GAPDH was localized mainly in the nucleus. Thus, the subcellular localization and expression level of endogenous GAPDH was different between neuronal and non-neuronal cell lines.

We have clearly shown that control NB41A3 cells, despite the fact that GAPDH displays nuclear localization, were not apoptotic, so the presence of GAPDH in the nucleus does not induce apoptosis per se. This observation challenges earlier propositions that nuclear localization alone might be an early indication of apoptotic cells or might even be responsible for apoptosis (Epner et al., 1999; Ishitani et al., 1998; Saunders et al., 1997; Saunders et al., 1999; Sawa et al., 1997; Shashidharan et al., 1999; Tajima et al., 1999). Nevertheless, the increased levels of nuclear GAPDH measured 24 hours after induction of apoptosis by MG132 or staurosporine in both cell lines, NB41A3 and R6, indicate that there may be a correlation between translocation of GAPDH into the nucleus and programmed cell death. In addition, neuroblastoma NB41A3 cells seem more resistant to apoptosis as only 20% of NB41A3 cells were apoptotic (a ratio similar to that found for R6-Bcl2 cells), compared with 50% (staurosporine treated) or 70% (MG132 treated) apoptotic cells in R6 fibroblasts.

Bcl2 prevents nuclear translocation of endogenous GAPDH during apoptosis but not in oxidative stress

Furthermore, nuclear translocation is three times lower in R6-Bcl2 cells than in R6 cells, indicating that Bcl2 does protect cells from apoptosis as described previously (Allen et al., 1998; Chao and Korsmeyer, 1998), and also that Bcl2 efficiently prevents translocation of endogenous GAPDH into the nucleus. Bcl2-mediated inhibition of GAPDH translocation may be part of its mechanism of protection against apoptosis. Most cells that display nuclear GAPDH translocation do not have a fragmented nucleus or show membrane blebbing. Therefore, translocation may be an early event in the apoptotic cascade, most probably before the point of no return, where the cell death program can no more be stopped.

Overexpression of GAPDH-GFP raises its nuclear localization in R6 cells and in transiently or stably transfected NB41A3 cells. This is a specific phenomenon and not a side-effect, because cells transfected with GFP alone or with (for example) enolase-GFP show neither nuclear translocation nor increased apoptosis (Z. Dastoor, PhD thesis, University of Fribourg, Switzerland, 2000). In some cases, GAPDH-GFP (besides being translocated from the cytoplasm into the nucleus) also accumulated in intracellular speckles or in extracellular membrane blebs and spikes. It is not very likely that formation of intracellular GAPDH-positive speckles may just be nonspecific aggregation of proteins, as this formation of speckles is never observed in resting cells or in cells that only express GFP. The mechanism of intracellular trafficking of GAPDH to its subcellular localization also remains to be further investigated.

Changes in GAPDH expression after induction of apoptosis and after oxidative stress

GAPDH-GFP transfected cells are more susceptible to apoptosis than untransfected cells and 10% are apoptotic per se. Not only are the numbers of cells showing chromatin condensation and nuclear fragmentation increased, but the percentage of cells displaying nuclear GAPDH-GFP localization or forming blebs and speckles is also increased significantly after exposure to staurosporine or MG132, compared with untransfected cells. Transient overexpression of GAPDH-GFP in R6-Bcl2 cells shows the same effects as in R6 cells. Thus, Bcl2 efficiently decreases nuclear translocation and apoptosis in untransfected cells, but has no effects when GAPDH-GFP is overexpressed, either in cells at rest or in cells exposed to apoptotic agents.

Different stages of translocation of endogenous GAPDH can be distinguished in R6 fibroblasts after exposure to apoptotic agents. First, GAPDH is localized in the perinuclear area of flat, typically fibroblast-shaped cells with a clear cytoskeletal structure; then it is translocated into the nucleus. Although the cytoplasmic structure of the cytoskeleton was not clearly visible anymore, the fibroblasts had not changed their morphology and their nuclei were not fragmented. At the next stage, cells are typical apoptotic, displaying cell shrinkage and nuclear fragmentation, and overexpress high amounts (three times more than basal levels) of GAPDH around the fragmented nuclei. The cells are rounded up and have no processes. In a final step, no GAPDH is visible anymore. In NB41A3 cells and in cells that overexpress GAPDH-GFP, these steps are similar, but a significant amount of GAPDH is found in the nucleus already before exposure to apoptotic drugs. The first two steps are also observed after oxidative stress, including nuclear translocation, but the cells do not undergo subsequent apoptosis.

Increased GAPDH expression at very high levels, which is observed in apoptotic cells, proceeds together with nuclear fragmentation. GAPDH does not seem bound to the DNA at this stage, as it is found nearly everywhere except where fragmented nucleus is detected. These cells have shrunk and are rounded up. It can be speculated that the loss of specific cell shape and of processes may be due to the loss of GAPDH tubulin bundling activity in the cytoplasm. At the final stage only the fragmented nucleus can be seen, but no visible GAPDH is found in the cell.

Our results demonstrate the role of GAPDH not only in apoptosis, but also in response to oxidative stress and differential GAPDH translocation in neuronal compared with non-neuronal cells. NB41A3 neuroblastoma cells are less sensitive than R6 fibroblasts to pro-apoptotic agents and to reagents that induce oxidative stress. Within 2 hours of exposure to either 100 μM H_2O_2 or 300 μM FeCN, endogenous GAPDH was translocated into the nucleus in untransfected R6 and NB41A3 cells, but no increase in nuclear fragmentation over control cells was observed. In addition, transfection of GAPDH-GFP per se (without induction of oxidative stress) already slightly enhances nuclear levels of the protein. In contrast to its protective effects during apoptosis, Bcl2 has no influence in response to oxidative stress, regardless of whether cells were transfected with GAPDH-GFP or not. So nuclear translocation of GAPDH may be mechanistically different between apoptosis and oxidative stress. Our observation that overexpressed Bcl2 in R6 cells had no effects on GAPDH translocation after oxidative stress, does not support direct linking of Bcl2 to the antioxidant pathway (Chao and Korsmeyer, 1998).

Relevance of nuclear translocation to GAPDH function

Changes in subcellular localization may be associated with

various post-translational modifications (phosphorylation or ADP ribosylation), which lead to changes in GAPDH activity and function, as suggested from other studies (Mezquita et al., 1998; Glaser and Gross, 1995; Soukri et al., 1996). Nuclear GAPDH could act as a nuclear RNA transport protein in nuclear RNA export (Singh and Green, 1993), as a post-transcriptional regulatory *cis*-element (Zhang et al., 1998) or as a uracil DNA glycosylase (UDG) with DNA repair activity (Arenaz and Sirover, 1983; Vollberg et al., 1989). However GAPDH-mediated tRNA export has no impact to apoptosis (Sawa et al., 1997). However, although GAPDH concentration increases in the nucleus of apoptotic cells, the UDG activity is lower than in control cells (Saunders et al., 1999). Despite increasing evidence that GAPDH is involved in apoptosis, its role is unclear. It may be related to changes in the levels of $A_{p3}A/A_{p4}A$ (Vartanian et al., 1999) or of glutathione, which are observed during apoptosis (Zhao et al., 1997) and GAPDH could then function as an Ap4A- or glutathione-binding protein.

GAPDH may serve as a nuclear carrier in apoptosis

Our results strongly indicate that it is not the nuclear localization of GAPDH itself, but rather an event coupled to the import of GAPDH into the nucleus that is responsible for the apoptotic action of GAPDH. We have shown under various different conditions that GAPDH is found at high levels in the nucleus, without inducing or enhancing apoptosis. Therefore, in agreement with earlier studies (Katsube et al., 1999; Sawa et al., 1997), we propose that GAPDH functions as a molecular chaperone, acting as a pro-apoptotic enzyme downstream of Bcl2 in the cell signal transduction cascade of apoptosis. Its nuclear translocation in combination with other factors may be a key event during apoptosis and could have an influence in several neurodegenerative diseases. Selective binding of GAPDH to gene products of different neurodegenerative diseases is well established, e.g. binding to huntingtin in Huntington's disease (HD), to atrophin in dentatorubropallidoluysian atrophy (Burke et al., 1996), to ataxin in spinocerebellar ataxia type 1, to the androgen receptor in spinobulbar muscular atrophy (Koshy et al., 1996), to ataxin 3 in Machado-Joseph disease (Paulson et al, 1997) or to the β-amyloid precursor protein in Alzheimer's disease (Schulze et al., 1993). The N-terminal fragments of huntingtin and ataxin are located into intranuclear inclusions in neurons of affected brain regions (DiFiglia et al., 1997; Paulson et al., 1997), supporting the view that GAPDH could serve as a carrier to mediate their nuclear translocation.

The authors are indebted to Mrs C. Deforel-Poncet and Mrs A. Hayoz for skilled technical assistance, to Dr M. Celio and Dr M. Ibrahim for their invaluable help in the immunocytochemical studies, to Dr S. Rusconi and Dr S. Brenz-Verca for their help in molecular biology, and to Dr C. Borner for supplying R6-Bcl2 cell lines and his advice. This work was supported by a grant No. 31-53206.97 from the Swiss National Foundation.

REFERENCES

Allen, R. T., Cluck, M. W. and Agrawal, D. K. (1998). Mechanisms controlling cellular suicide: role of Bcl-2 and caspases. *Cell Mol Life Sci.* **54**, 427-445.

Arcari, P., Martinelli, R. and Salvatore, F. (1989) *Biochem. Genet*. **27**, 439-450.

Arenaz, P. and Sirover, M. A. (1983). Isolation and characterization of monoclonal antibodies directed against the DNA repair enzyme uracil DNA glycosylase from human placenta. *Proc. Natl. Acad. Sci. USA* **80**, 822-826.

Ashmarina, L. I., Louzenko, S. E., Severin, S. E., Muronetz., V. I. and Nagradova, N. K. (1988). Phosphorylation of D-glyceraldehyde-3-phosphate dehydrogenase by Ca2+/calmodulin-dependent protein kinase II. *FEBS Lett.* **231**, 413-416.

Augusti-Tocco, G. and Sato, G. (1969). Establishment of functional clonal lines of neurones from mouse neuroblastoma. *Proc. Natl. Acad. Sci. USA* **64**, 311-315.

Baxi, M. D. and Vishwanatha, J. K. (1995). Uracil DNA-glycosylase/glyceraldehyde-3-phosphate dehydrogenase is an Ap4A binding protein. *Biochemistry* **34**, 9700-9707.

Borner, C. (1996). Diminished Cell Proliferation associated with the Death-protective activity of Bcl-2. *J. Biol. Chem.* **271**, 12695-12698.

Brune, B. and Lapetina, E. G. (1996). Nitric oxide-induced covalent modification of glycolytic enzyme glyceraldehyde-3-phosphate dehydrogenase. *Methods Enzymol.* **269**, 400-407.

Bulliard, C., Zurbriggen, R., Tornare, J., Faty, M., Dastoor, Z. and Dreyer. J. L. (1997). Purification of a dichlorophenol-indophenol oxidoreductase from rat and bovine synaptic membranes, tight complex association of a glyceraldehyde-3-phosphate dehydrogenase isoform, TOAD64, enolase-γ and aldolase C. *Biochem J.* **324**, 555-563.

Burke, J. R., Enghild, J. J., Martin, M. E., Jou, Y. S., Myers, R. M., Roses, A. D., Vance, J. M. and Strittmatter, W. J. (1996). Huntingtin and DRPLA proteins selectively interact with the enzyme GAPDH. *Nat. Med.* **2**, 347-350.

Chao, D. T. and Korsmeyer, S. J. (1998). Bcl-2 family: regulators of cell death. *Annu. Rev. Immunol.* **16**, 395-419.

Cooper, A. J. L., Sheu, K. R., Burke, J. R., Onodera, O., Strittmatter, W. J., Roses, A. D. and Blass, J. P. (1997). Transglutaminase-catalyzed inactivation of glyceraldehyde-3-phosphate dehydrogenase and α-ketoglutarate dehydrogenase complex by polyglutamine domains of pathological length. *Proc. Natl. Acad. Sci. USA* **94**, 12604-12609.

Dastoor, Z. and Dreyer, J.-L. (2000) Nuclear trasnlocation and aggregate formation of heat shock cognate protein 70 (Hsc70) in oxidative stress and apoptosis. *J. Cell Sci.* **113**, 2845-2854

DiFiglia, M., Sapp, E., Chase, K., ODavies, S. W., Bates, G. P., Vonsattel, J. P. and Aronin, N. (1997). Aggregation of huntingtin in neuronal intranuclear inclusions and dystrophic neurites in brain. *Science.* **277**, 1990-1993.

Durrieu, C., Bernier-Valentin, F. and Rousset, B. (1987). Microtubules bind glyceraldehyde-3-phosphate dehydrogenase and modulate its enzyme activity and quaternary structure. *Arch. Biochem. Biophys.* **252**, 32-40.

Epner, D. E., Sawa, A. and Isaacs, J. T. (1999). Glyceraldehyde-3-phosphate dehydrogenase expression during apoptosis and proliferation of rat ventral prostate. *Biol. Reprod.* **61**, 687-691.

Glaser, P. E. and Gross, R. W. (1995). Rapid plasmenylethanolamine-selective fusion of membrane bilayers catalyzed by an isoform of glyceraldehyde-3-phosphate dehydrogenase: discrimination between glycolytic and fusogenic roles of individual isoforms. *Biochemistry* **34**, 12193-121203.

Hessler, R. J., Blackwood, R. A., Brock, T. G., Francis, J. W., Harsh, D. M. and Smolen, J. E. (1998). Identification of glyceraldehyde-3-phosphate dehydrogenase as a Ca^{2+}- dependent fusogen in human neutrophil cytosol. *J. Leukoc. Biol.* **63**, 331-336.

Ishitani, R., Sunaga, K., Hirano, A., Saunders, P., Katsube, N. and Chuang, D. M. (1996). Evidence that glyceraldehyde-3-phosphate dehydrogenase is involved in age-induced apoptosis in mature cerebellar neurones in culture. *J. Neurochem.* **66**, 928-935.

Ishitani, R., Tanaka, M., Sunaga, K., Katsube, N. and Chuang, D. M. (1998). Nuclear localization of overexpressed glyceraldehyde-3-phosphate dehydrogenase in cultured cerebellar neurones undergoing apoptosis. *Mol. Pharmacol.* **53**, 701-707.

Katsube, N., Sunaga, K., Aishita, H., Chuang, D. M. and Ishitani, R. (1999). ONO-1603, a potential antidementia drug, delays age-induced apoptosis and suppresses overexpression of glyceraldehyde-3-phosphate dehydrogenase in cultured central nervous system neurones. *J. Pharmacol. Exp. Ther.* **288**, 6-13.

Kawamoto, R. M. and Caswell, A. H. (1986). Autophosphorylation of glyceraldehydephosphate dehydrogenase and phosphorylation of protein from skeletal muscle microsomes. *Biochemistry* **25**, 657-661.

Koshy, B., Matilla, T., Burright, E. N., Merry, D. E., Fischbeck, K. H., Orr, H. T. and Zoghbi, H. Y. (1996). Spinocerebellar ataxia type-1 and spinobulbar muscular atrophy gene products interact with glyceraldehyde-3-phosphate dehydrogenase. *Hum. Mol. Genet.* **5**, 1311-1318.

Meyer-Siegler, K., Mauro, D. J., Seal, G., Wurzer, J., deRiel, J. K. and Sirover, M. A. (1991). A human nuclear uracil DNA glycosylase is the 37-kDa subunit of glyceraldehyde-3-phosphate dehydrogenase. *Proc. Natl. Acad. Sci. USA* **88**, 8460-8464.

Mezquita, J., Pau, M. and Mezquita, C. (1998). Several novel transcripts of glyceraldehyde-3-phosphate dehydrogenase expressed in adult chicken testis. *J. Cell Biochem.* **71**, 127-139.

Morgenegg, G., Winkler, G. C., Hubscher, U., Heizmann, C. W., Mous, J. and Kuenzle, C. C. (1986). Glyceraldehyde-3-phosphate dehydrogenase is a nonhistone protein and a possible activator of transcription in neurones. *J. Neurochem.* **47**, 54-62.

Muronetz, V. I., Wang, Z. X., Keith, T. J., Knull, H. R. and Srivastava, D. K. (1994). Binding constants and stoichiometries of glyceraldehyde 3-phosphate dehydrogenase-tubulin complexes. *Arch. Biochem. Biophys.* **313**, 253-260.

Nagy, E. and Rigby, W. F. (1995). Glyceraldehyde-3-phosphate dehydrogenase selectively binds AU-rich RNA in the NAD(+)-binding region (Rossmann fold). *J. Biol. Chem.* **270**, 2755-2763.

Paulson, H. L., Perez, M. K., Trottier, Y., Trojanowski, J. Q., Subramony, S. H., Das, S. S., Vig, P., Mandel, J. L., Fischbeck, K. H. and Pittman, R. N. (1997). Intranuclear inclusions of expanded polyglutamine protein in spinocerebellar ataxia type 3. *Neuron.* **19**, 333-344.

Reiss, N., Hermon, J., Oplatka, A. and Naor, Z. (1996a). Interaction of purified protein kinase C with key proteins of energy metabolism and cellular motility. *Biochem. Mol. Biol. Int.* **38**, 711-719.

Saunders, P. A., Chalecka-Franaszek, E. and Chuang, D. M. (1997). Subcellular distribution of glyceraldehyde-3-phosphate dehydrogenase in cerebellar granule cells undergoing cytosine arabinoside-induced apoptosis. *J. Neurochem.* **69**, 1820-1828.

Saunders, P. A., Chen, R. W. and Chuang, D. M. (1999). Nuclear translocation of glyceraldehyde-3-phosphate dehydrogenase isoforms during neuronal apoptosis. *J. Neurochem.* **72**, 925-932.

Sawa, A., Khan, A. A., Hester, L. D. and Snyder, S. H. (1997). Glyceraldehyde-3-phosphate dehydrogenase: nuclear translocation participates in neuronal and nonneuronal cell death. *Proc. Natl. Acad. Sci. USA* **94**, 11669-11674.

Schultz, D. E., Hardin, C. C. and Lemon, S. M. (1996). Specific interaction of glyceraldehyde 3-phosphate dehydrogenase with the 5′-nontranslated RNA of hepatitis A virus. *J. Biol. Chem.* **271**, 14134-14142.

Schulze, H., Schuler, A., Stuber, D., Dobeli, H., Langen, H. and Huber, G. (1993). Rat brain glyceraldehyde-3-phosphate dehydrogenase interacts with the recombinant cytoplasmic domain of Alzheimer's β-amyloid precursor protein. *J. Neurochem.* **60**, 1915-1922.

Shashidharan, P., Chalmers-Redman, R. M., Carlile, G. W., Rodic, V., Gurvich, N., Yuen, T., Tatton, W. G. and Sealfon, S. C. (1999). Nuclear translocation of GAPDH-GFP fusion protein during apoptosis. *NeuroReport* **10**, 1149-1153.

Singh, R. and Green, M. R. (1993). Sequence-specific binding of transfer RNA by glyceraldehyde-3-phosphate dehydrogenase. *Science* **259**, 365-368.

Soukri, A., Hafid, N., Valverde, F., Elkebbaj, M. S. and Serrano, A. (1996). Evidence for a posttranslational covalent modification of liver glyceraldehyde-3-phosphate dehydrogenase in hibernating jerboa (Jaculus orientalis). *Biochim. Biophys. Acta.* **1292**, 177-187.

Sunaga, K., Takahashi, H., Chuang, D. M. and Ishitani, R. (1995). Glyceraldehyde-3-phosphate dehydrogenase is over-expressed during apoptotic death of neuronal cultures and is recognized by a monoclonal antibody against amyloid plaques from Alzheimer's brain. *Neurosci Lett.* **200**, 133-136.

Tajima, H., Tsuchiya, K., Yamada, M., Kondo, K., Katsube, N. and Ishitani, R. (1999). Over-expression of GAPDH induces apoptosis in COS-7 cells transfected with cloned GAPDH cDNAs. *NeuroReport* **10**, 2029-2033.

Vartanian, A., Alexandrov, I., Prudowski, I., McLennan, A. and Kisselev, L. (1999). Ap4A induces apoptosis in human cultured cells. *FEBS Lett.* **456**, 175-180.

Vollberg, T. M., Siegler, K. M., Cool, B. L. and Sirover, M. A. (1989). Isolation and characterization of the human uracil DNA glycosylase gene. *Proc. Natl. Acad. Sci. USA* **86**, 8693-8697.

Yong, Y. and Dreyer, J. L. (1995). Distribution of six transplasma membrane NADH-dehydrogenases in rat brain tissue. *Dev. Brain Res.* **89**, 235-252.

Zhang, W. Q., Fieno, A. M., Grant, R. A. and Yen, T. S. (1998). Identification of glyceraldehyde-3-phosphate dehydrogenase as a cellular protein that binds to the hepatitis B virus post-transcriptional regulatory element. *Virology* **248**, 46-52

Zhao, Z., Francis, C. E., Welch, G., Loscalzo, J. and Ravid, K. (1997). Reduced glutathione prevents nitric oxide-induced apoptosis in vascular smooth muscle cells. *Biochim. Biophys. Acta.* **1359**, 143-152.

Zurbriggen, R. and Dreyer, J. L. (1996). The plasma membrane NADH-diaphorase is active during selective phases of the cell cycle in mouse neuroblastoma cell line NB41A3. Its relation to cell growth and differentiation. *Biochim. Biophys. Acta.* **1312**, 215-222.